ARTICLE

doi:10.1038/nature11045

Clonally dominant cardiomyocytes direct heart morphogenesis

Vikas Gupta[1] & Kenneth D. Poss[1]

As vertebrate embryos develop to adulthood, their organs undergo marked changes in size and tissue architecture. The heart acquires muscle mass and matures structurally to fulfil increasing circulatory needs, a process that is incompletely understood. Here we used multicolour clonal analysis to define the contributions of individual cardiomyocytes as the zebrafish heart undergoes morphogenesis from a primitive embryonic structure into its complex adult form. We find that the single-cardiomyocyte-thick wall of the juvenile ventricle forms by lateral expansion of several dozen cardiomyocytes into muscle patches of variable sizes and shapes. As juvenile zebrafish mature into adults, this structure becomes fully enveloped by a new lineage of cortical muscle. Adult cortical muscle originates from a small number of cardiomyocytes—an average of approximately eight per animal—that display clonal dominance reminiscent of stem cell populations. Cortical cardiomyocytes initially emerge from internal myofibres that in rare events breach the juvenile ventricular wall, and then expand over the surface. Our results illuminate the dynamic proliferative behaviours that generate adult cardiac structure, revealing clonal dominance as a key mechanism that shapes a vertebrate organ.

Vertebrate organ development is an intricate process that begins in the early embryo and continues until the functional capacity of the organ meets adult requirements. Relatively little is known about the cellular mechanisms of organ morphogenesis after birth or hatching. This can be explained in part by the challenges of analysing dynamic cellular behaviours in complex tissues.

New technologies can shed light on the cellular mechanisms that drive organ morphogenesis. Recently, a system was developed that allowed the designation of ~90 colour labels to murine neurons[1]. With this technology, termed Brainbow, it was possible to visualize adjacent neurons and their connections in the brain with high resolution. The ability to assign many colours to different cells in a population can also be applied to investigating cell proliferation and lineage decisions.

The heart is a set of chambers comprised predominantly of the contractile units, cardiomyocytes. Genetic fate mapping has been performed to determine how separate lineages contribute to developing cardiac structures in mice and zebrafish[2–6]. Additionally, single-marker clonal analysis has traced the activity of individual cells during embryonic heart patterning[7–10]. These studies have enhanced our understanding of cardiogenic mechanisms in early embryos. Nevertheless, a large gap in our knowledge remains in comprehending how the size, shape and structure of an adult heart are finalized through the individual and population behaviours of many cardiac cells.

In this study, we used multicolour clonal analysis to map the proliferative histories of many individual cardiomyocytes as the zebrafish cardiac ventricle transitions from a simple tube of single-cardiomyocyte thickness into a complex adult structure. Our experiments yielded several unexpected discoveries relevant to the number, nature and mechanisms of cardiomyocyte contributions during heart morphogenesis.

Multicolour labelling of cardiomyocytes

To study cell clones in zebrafish, we adapted the Brainbow 1.0L construct for combinatorial expression of three spectrally different fluorescent reporter proteins[1]. Multiple copy integration of this transgene at a single genetic locus is a common outcome of transgenesis. Thus, combinatorial Cre-recombinase-mediated excision events at paired *lox* recognition sites can generate many possible permanent colours (Fig. 1a, b). We generated several transgenic lines containing a *β-actin-2*-promoter-driven multicolour construct, and assessed them in combination with a strain harbouring a tamoxifen-inducible, cardiomyocyte-restricted Cre recombinase, *cmlc2:CreER*[11]. We identified one line, *Tg(β-act2:Brainbow1.0L)*^{pd49} (referred to subsequently as *priZm*), showing limited mosaic recombination only in the presence of 4-hydroxytamoxifen (4-HT; Supplementary Fig. 1).

The size and structure of the zebrafish heart is conducive to clonal analysis of cardiomyocytes. The 2–3 days post-fertilization (dpf) zebrafish heart is looped, has a wall of single-cardiomyocyte thickness, and consists of 250–300 muscle cells; by our measurements ~115 of these are contained within the ventricular wall (Supplementary Fig. 2). Cardiomyocyte proliferation is detectable at 2 dpf and is thought to account for most or all subsequent cardiogenesis[2,12–15]. To trace the fates of individual embryonic cardiomyocytes, we briefly incubated 2 dpf *cmlc2:CreER*; *priZm* embryos in 4-HT and raised them to different ages (Fig. 1c).

We first assessed cardiac fluorescence at 10 dpf, a stage comparable in organismal size to 2 dpf. Our optimized 4-HT regimen generated >20 unique colours in cardiomyocytes, as viewed at 10 dpf and subsequent stages. Red fluorescent protein (RFP) is the initial reporter cassette and default expression marker, and 4-HT treatment induced recombination (non-red colours) in ~50% of ventricular cardiomyocytes. Importantly, different colours were consistently assigned to adjacent cardiomyocytes on the surface of the 10 dpf ventricular wall (Fig. 1d–f and Supplementary Fig. 3), a prerequisite for multicolour clonal analysis.

The zebrafish ventricle is recognized to contain two types of cardiac muscle[16]. These include a peripheral wall of compact muscle, and inner myofibres organized into trabeculae that initiate formation at 3 dpf (ref. 17). Histological examination of 10 dpf hearts revealed three notable observations. First, the ventricular wall remained at single-cardiomyocyte thickness, as at 2 dpf. Second, trabecular myocytes

[1]Department of Cell Biology and Howard Hughes Medical Institute, Duke University Medical Center, Durham, North Carolina 27710, USA.

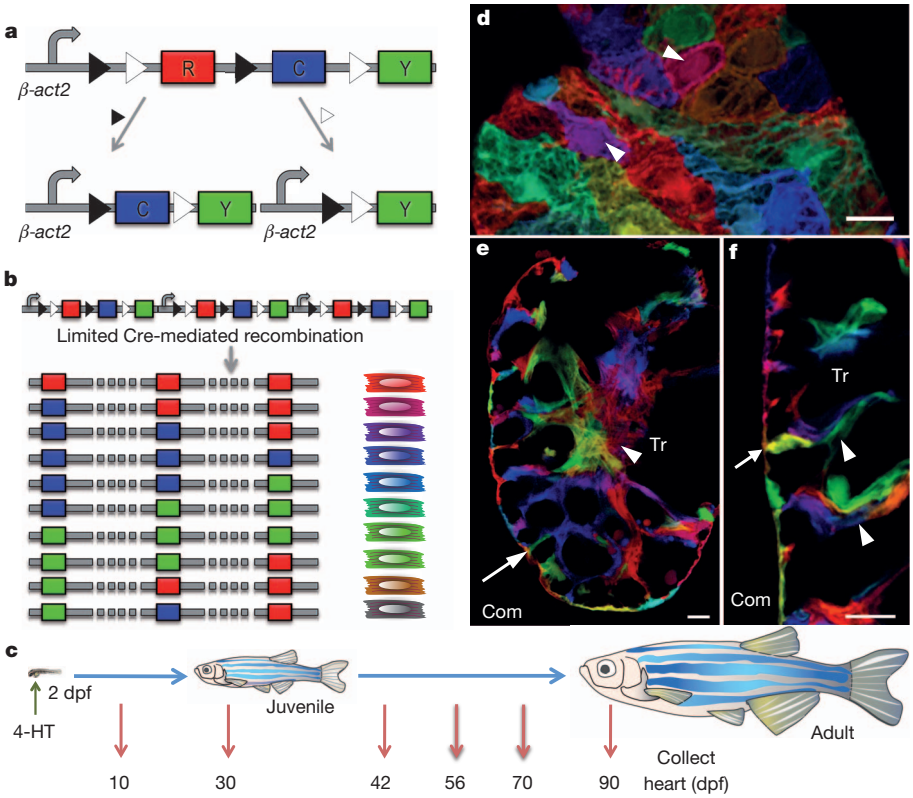

Figure 1 | Multicolour clonal labelling of embryonic zebrafish cardiomyocytes. **a**, Recombination at paired *lox2272* (black triangles) or *loxP* (white triangles) sites leads to expression of cyan fluorescent protein (CFP) or yellow fluorescent protein (YFP), respectively. **b**, Limited Cre-mediated recombination of tandem cassette insertions results in combinatorial expression of fluorescent proteins. **c**, Cartoon of lineage-tracing experiments. **d**, 10 dpf ventricular surface myocardium. Single cardiomyocytes are predominantly labelled with unique colours (arrowheads). **e**, **f**, 10 dpf ventricular confocal slice, indicating trabecular cardiomyocytes connected with clonally unrelated cardiomyocytes at the wall (**e**, **f**, arrow) and within trabeculae (**f**, arrowheads). Com, compact muscle; Tr, trabecular muscle. Scale bars, 10 μm.

connected to the wall were most often clonally unrelated to adjoining wall myocytes (58 of 63 observations, $n = 5$ ventricles; Fig. 1e, f). This observation supported a mechanism for trabecularization proposed recently based on different lines of evidence, in which myocytes delaminate from the ventricular wall, seed elsewhere in the chamber, and initiate trabecular growth from a second site[17]. Third, we saw that the trabecular myofibres themselves were comprised of cardiomyocytes arising from different clonal origins within the 2 dpf wall (Fig. 1f).

Juvenile ventricular wall formation

We next examined the ventricles of juvenile zebrafish at 30 dpf, at which time major organismal and cardiac growth have occurred since cardiomyocyte labelling with 4-HT. By whole-mount imaging of surface myocardium, we readily identified multicellular, single-colour regions of myocardium, indicating that progeny of embryonic cardiomyocytes generally remained connected with one another after division (Fig. 2a–c and Supplementary Fig. 4a–c). Although less common (9.8% of clones), we also observed instances suggesting complete separation of a cardiomyocyte from its clonal partners (Supplementary Fig. 4d).

We expected some uniformity to the clonal patches comprising the ventricular wall, with cardiomyocyte clones of similar shape and size. By contrast, ventricles from different animals displayed unique patterns of surface colour clones, and the shapes of clones within each ventricle were highly diverse (Fig. 2a and Supplementary Fig. 5). Clone size also varied. Some clones showed evidence of many cell divisions, whereas others contained a single cardiomyocyte (Fig. 2d). Histological analysis showed retention of a wall of single-cardiomyocyte thickness, indicating that the expansion of wall clones was limited to lateral directions along the surface. They also revealed that substantial expansion of trabecular myocardium had occurred since 10 dpf (Fig. 2e).

To estimate the number of embryonic cardiomyocytes that create the juvenile ventricular wall, we calculated the surface areas occupied by individual clones and divided each by the total ventricular surface area. Most clones (99/146; $n = 5$) each occupied less than 2% of the ventricular surface area, whereas a small number (15/146) of larger clones each represented ~4–8% of the surface (Fig. 2f). Extrapolating for unrecombined myocardium, we determined that the 30 dpf ventricular surface was represented by 55.4 ± 1.9 colour clones ($n = 10$; mean ± standard error of the mean (s.e.m.); Fig. 2g). Thus, our data indicate that the juvenile zebrafish ventricular wall is built by lateral expansion of ~55 embryonic cardiomyocytes. These cardiogenic events create a patchwork of diverse clonal shapes and sizes that varies from animal to animal, indicating that the juvenile cardiac form can be acquired with considerable developmental plasticity.

Emergence of a new adult muscle lineage

Zebrafish are typically recognized as adults at 3 months post-fertilization. We examined ventricles of 6-, 8- and 10-week-old animals that had undergone cardiomyocyte labelling at 2 dpf. At 6 weeks post-fertilization (wpf), most clonal patches comprising the surface myocardium appeared similar to those of 30 dpf ventricles. Additionally, we detected a population of clonally related cardiomyocytes layered upon these patches near the chamber base (Fig. 3a, b). By 8 wpf, large single-colour swaths containing several hundreds of such cardiomyocytes extended from the ventricular base, wrapping around both sides of the chamber and often reaching its midpoint (Fig. 3d–f). At 10 wpf, we began to see evidence of these surface clones converging with each other. These external cardiomyocytes were typically more rod-shaped with more distinct striation than underlying cardiomyocytes (Supplementary Fig. 6).

We examined histological sections and confocal slices through ventricles from 6–10 wpf animals, which confirmed that a new layer

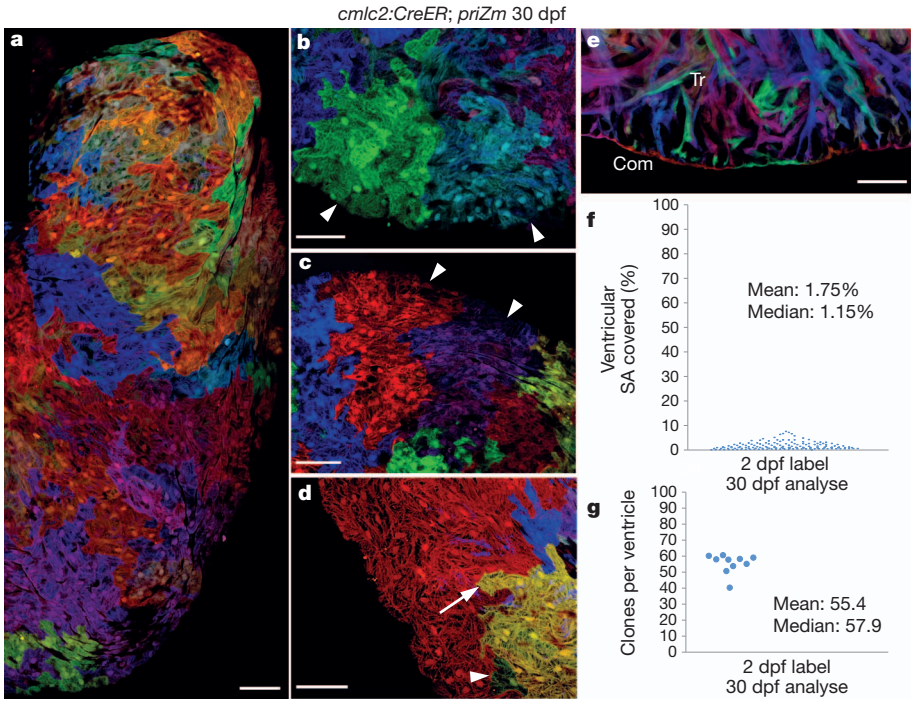

Figure 2 | Several dozen embryonic cardiomyocytes build the juvenile ventricular wall. **a**, Surface myocardium of half of a 30 dpf ventricular side, displaying clonal patches of varied shapes and sizes. **b**, **c**, Cardiomyocyte clones near the apex or chamber midpoint forming wedge/stripe shapes (arrowheads). **d**, Single-cell clone (green, arrowhead) positioned near a large clone (yellow, arrow). **e**, 30 dpf ventricular confocal slice, depicting a wall of single-cardiomyocyte thickness (Com) surrounding trabecular muscle (Tr). **f**, Percentage surface area (SA) occupied by 30 dpf clones (146 clones, 5 ventricles). **g**, Surface clones per ventricle ($n = 10$). Scale bars, 50 μm.

of ventricular muscle had emerged externally to the wall of single-cardiomyocyte thickness present at earlier stages (Fig. 3c, g). As indicated by whole-mount imaging, this external layer typically displayed substantial regions of clonally related cardiomyocytes. We will refer subsequently to the inner wall muscle as the 'primordial layer', as it retains the same single-cardiomyocyte thickness and characteristics

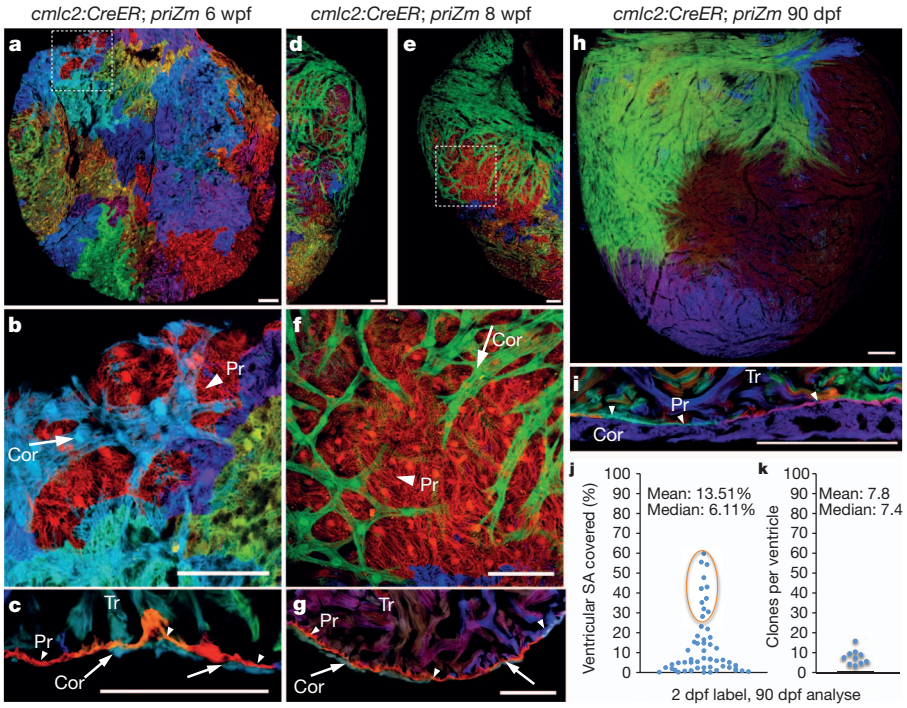

Figure 3 | Clonally dominant cortical cardiomyocytes. **a**–**c**, 6 wpf ventricular surface (**a**, **b**) and confocal slice (**c**), indicating cortical (Cor; arrow), primordial (Pr; arrowhead) and trabecular (Tr) muscle. **d**–**g**, 8 wpf ventricular surface indicating a large green basal clone (**d**–**f**), and section indicating 3 muscle types (**g**). Dashed boxes in **a** and **e** are shown in higher magnification in **b** and **f**, respectively. **h**, 90 dpf ventricular surface, showing only a few large cortical clones. **i**, 90 dpf ventricular section. **j**, Percentage surface area (SA) occupied by 90 dpf clones (56 clones, 10 ventricles); basal clones representing each ventricle are circled. **k**, Surface clones per ventricle ($n = 10$). Scale bars, 50 μm (**a**–**g**); 100 μm (**h**, **i**).

of the embryonic ventricle throughout subsequent life stages. We will refer to the late-emerging, outermost muscle of the ventricular wall as the 'cortical layer'. Thus, by multicolour clonal analysis, we revealed two developmentally distinct and previously unrecognized forms of ventricular wall myocardium.

Dominant clones build adult wall muscle

We next examined ventricles from mature, 90 dpf zebrafish that had undergone cardiomyocyte labelling at 2 dpf. At this stage, the entire surface of the ventricle in each animal was covered by cortical cardiomyocytes (Fig. 3h and Supplementary Fig. 7). Similar to the clonal representation of the primordial layer at earlier stages, cortical clone patterns appeared different in each animal. However, a common theme for each ventricle was the presence of one or two large cortical clones at the base of the heart extending across the ventricular surface towards the apex. We infer from our time-point analysis that these areas of cortex formed by a base-to-apex wave of expansion over the primordial layer. A number of smaller surface clones were apparent at other locations. Clones converged by weaving or fitting with some overlay into each other, and were penetrated by coronary vessels (Supplementary Fig. 8).

Histological analysis of adult ventricular tissue indicated that the primordial layer remained at single-cardiomyocyte thickness and was comprised of multiple colour clones. This appearance contrasted with the overlying cortical myocardium, which was predominantly single colour and could be several cells thick (Fig. 3i). We calculated the areas of surface clones from whole-mount images of ventricles that displayed basal clones of a recombined colour. Ten of twenty ventricles met this criterion, each of which had a large cortical clone covering 30–60% of the total ventricular surface (Fig. 3j). An average of 7.8 ± 1.2 clones contributed the entire cortical muscle of each ventricle ($n = 10$; Fig. 3k), a number several times lower than the clonal surface representation of the much smaller juvenile ventricle. Thus, a rare group of approximately eight clonally dominant cardiomyocytes in the embryonic ventricle ultimately contribute to building the adult cortical myocardium.

Muscle lineage regeneration after injury

Zebrafish possess a robust capacity for heart regeneration throughout life[18], based on the ability to activate the proliferation of spared cardiomyocytes after injury[11,19,20]. We examined the regenerative potentials of primordial and cortical muscle by amputating ventricular apices from 90 dpf *cmlc2:CreER*; *priZm* animals that had been labelled at 2 dpf. At 14 days post-amputation (dpa), we detected growth of adjacent cortical muscle clones in lateral and radial directions into the wound area (Fig. 4a, b), but the primordial layer lagged behind the amputation site. By 30 dpa, as the wall was reconstructed with clonal patches of cortical cardiomyocytes, clones of single-cardiomyocyte thickness contiguous with the primordial layer first became detectable in the regenerate (Fig. 4c). By 60 dpa, the primordial layer was largely restored as a complete structure positioned between cortical and trabecular muscle (Fig. 4d). Thus, regenerating primordial muscle undergoes restricted lateral expansion as during morphogenesis, whereas cortical muscle regeneration is less constrained and assumes the primary component of the new wall. Interestingly, these events occur in a temporally reversed manner compared to initial morphogenesis, with cortical muscle regenerating before the underlying primordial layer.

Origins of dominant cardiomyocyte clones

To determine when cortical cardiomyocytes originate during heart morphogenesis, we initiated colour labelling at 30 dpf, after formation of the juvenile structure but 1–2 weeks before the emergence of cortical muscle. Notably, large clonal patches were present on the surface of 90 dpf ventricles that had been incubated briefly with 4-HT at 30 dpf (Fig. 5a and Supplementary Fig. 9), with the largest clones

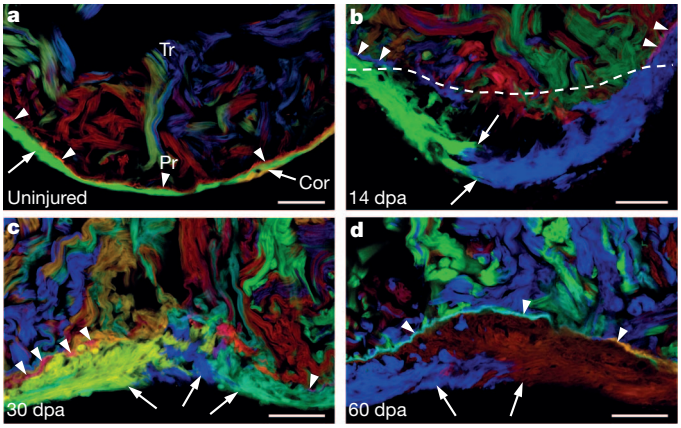

Figure 4 | Regeneration of cortical and primordial muscle after injury. **a**, Section of an uninjured ventricular apex, indicating the primordial (Pr; arrowheads) and cortical (Cor; arrows) layers. Tr, trabecular muscle. **b**, Regenerating ventricular apex at 14 days after resection (dpa). Cortical muscle clones converge within the injury site, whereas the primordial layer lags behind. Dashed line indicates amputation plane. **c**, 30 dpa ventricular apex, indicating multiple cortical clones and an incomplete primordial layer. **d**, Regenerated ventricular apex at 60 dpa, containing cortical muscle overlying a mostly contiguous layer of primordial muscle. $n = 6$ animals for each time point. Scale bars, 50 μm.

present at the chamber base. We quantified the size and number of clones in ventricles with basal clones of recombined colours (11 of 20 animals). Our data indicated that adult cortical myocardium arises in patches of diverse sizes from an average of 8.6 ± 0.7 labelled 30 dpf cardiomyocytes (Fig. 5b, c), a number similar to that observed after labelling at 2 dpf.

In some ventricles assessed 4 weeks after labelling (8 wpf), we observed trabecular muscle of the same colour near the emergent cortical clone (Fig. 5e, g). To confirm this association, we examined sections of 6–7 wpf ventricles (labelled at 2 dpf), and consistently found nearby trabecular muscle of the same colour as the small, basal cortical clone (13 of 13 ventricles; see cyan clone in Fig. 3c). We also could identify cases from these examples in which trabecular and cortical muscle of one colour connected through an apparent breach in the primordial layer (Supplementary Fig. 10). These observations suggested a clonal relationship between trabecular and cortical cardiomyocytes in the maturing zebrafish ventricle.

We noticed lower colour recombination in the primordial layer (~15%) than in the trabecular and cortical muscle lineages (~61%) at 8 wpf (Fig. 5d–g). Taking advantage of this differential labelling efficiency, we titrated 4-HT and identified a low dose that induced sparse recombination at 30 dpf in trabeculae and no obvious recombination in primordial muscle. Importantly, even with very limited labelling, cortical clones of a recombined colour were still discernable in 3 of 24 ventricles at 8 wpf (Fig. 5h, i), a finding that reaffirmed a trabecular source for the cortical lineage. As with other samples mentioned above, images of confocal slices from these ventricles could identify single-colour clones containing both cortical and trabecular muscle, connecting through an apparent breach in primordial muscle of unrecombined colour (Fig. 5i–k).

Together, our findings indicate a dynamic mechanism that generates a final ventricular muscle lineage and completes adult cardiac morphogenesis. Trabecular cardiomyocytes penetrate the primordial layer in rare, spatially segregated events at the juvenile stage, seed the ventricular surface, and undergo expansion to create the cortical myocardium.

Discussion

Multicolour clonal analysis enables the simultaneous fate mapping of many similar cells within a developing organ. We used this technology to reveal unsuspected cellular mechanisms guiding heart morphogenesis

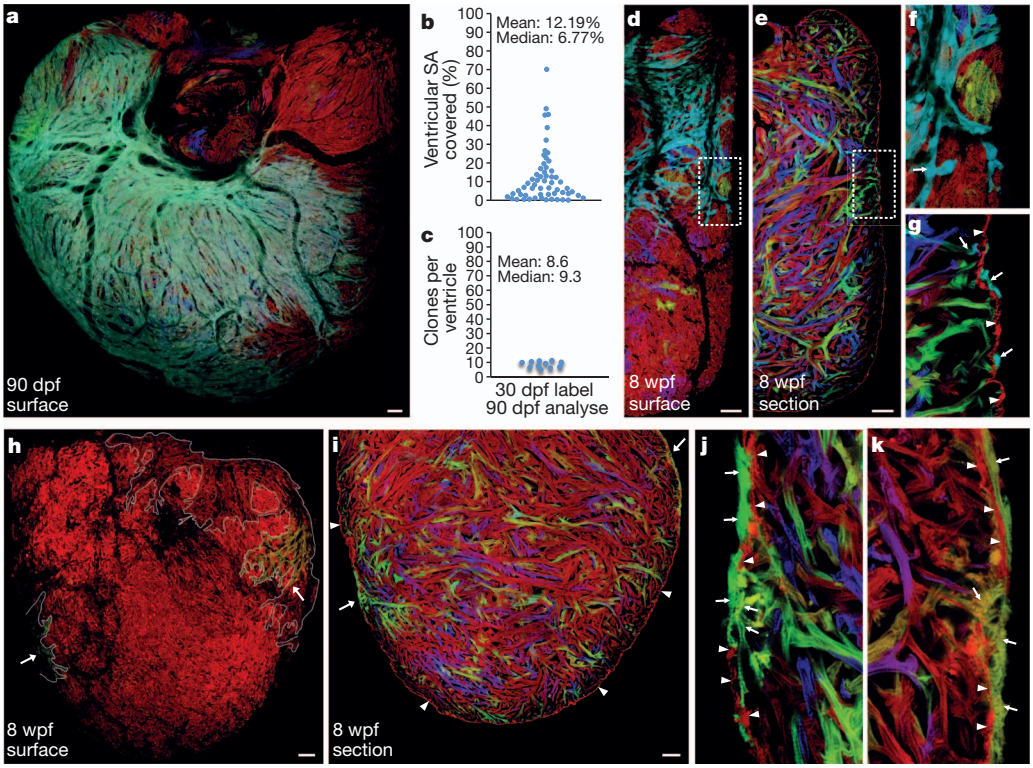

Figure 5 | Origins of clonally dominant cardiomyocytes. **a**, 90 dpf ventricular surface, after 30 dpf 4-HT labelling. **b**, Percentage surface area (SA) occupied by 90 dpf clones (58 clones, 11 ventricles). **c**, Surface clones per ventricle ($n = 11$). **d**–**g**, 8 wpf ventricular surface (**d**, **f**) and confocal slice (**e**, **g**), after 30 dpf 4-HT labelling. Cyan cortical muscle (arrows; **f**, **g**) overlies primordial muscle (arrowheads) that is largely red/unlabelled, and cyan trabeculae (arrow; **g**). Dashed boxes in **d** and **e** are shown at higher magnification in **f** and **g**, respectively. **h**–**k**, 8 wpf ventricular surface (**h**) and confocal slices (**i**–**k**) after limited 4-HT labelling, showing no obvious primordial muscle labelling (arrowheads; **i**–**k**). Arrows indicate green (**h**, **i** (left); **j**) and hazel (**h**, **i** (right); **k**) cortical/trabecular clones. All cortical muscle in **h** is outlined in white. Scale bars, 50 μm.

in zebrafish. We found that three ventricular myocardial lineages are present in the adult form: primordial, trabecular and cortical muscle, created in this order from each other. Our data indicate that the innermost trabecular lineage is initiated predominantly by delamination from the embryonic primordial layer and migration, as proposed in an earlier study[17]. Next, the outermost cortical layer is created as juveniles mature to adults, emerging wholly or in part via an 'inside-out' mechanism from trabeculae. Here, one or more particularly expansive juvenile cardiomyocytes access the ventricular surface at each of only approximately eight sites per animal.

Zebrafish share several aspects of cardiac development with higher vertebrates, and the multicolour clonal analysis results we report here indicate some basic commonalities with results of single-marker clonal analysis performed previously in early mouse and chick embryos. For instance, cardiomyocytes were also observed in coherent clonal populations during cardiac growth in these systems, after an early phase of dispersion[9,10]. Most unexpected is that the zebrafish ventricle maintains a primordial layer of single-cardiomyocyte thickness without noticeable cell division in the z-plane, and that wall thickening instead occurs after seeding of a separate cortical lineage by dominant clones. It will be interesting to determine the evolutionary distribution of aspects of this uncovered morphogenetic mechanism within other bony fish and among other classes of vertebrates like mammals.

The origins and diversity of clonal patterns of cortical muscle we report are more consistent with a stochastic model of source cell selection than a hierarchical or predetermined model. Additionally, the observation of clonal dominance in cardiomyocytes is reminiscent of stem cell compartments that drift towards clonality during homeostatic tissue maintenance, events that have been explained by stochastic models[21–24]. We suspect that molecular and/or physiological cues enable the emergence and proliferative capacity of cortical cardiomyocytes, ostensibly with a preferential influence at the ventricular base. It is likely that clonal dominance behaviour is a recurring mechanistic strategy to help shape vertebrate organs.

METHODS SUMMARY

Wild-type or transgenic zebrafish of the EK/AB background were used for all experiments. Ventricular resection surgeries were performed as described previously[18]. All published transgenic strains used here are listed in Methods and were analysed as hemizygotes. *Tg(β-act2:Brainbow1.0L)*^{pd49} was generated and 4-HT labelling experiments were performed as described in Methods. Hearts were extracted at the indicated time points and fixed in 4% paraformaldehyde. After rinsing, the atrium was removed and the ventricle was placed on a coverslip in Fluoromount G. Another coverslip was used to gently compress the ventricle, allowing imaging of both ventricular surfaces. For surface images of whole-mounted ventricles, the z-position was adjusted until only surface muscle was visible. For confocal slices through whole-mounted hearts, the z-position was adjusted through the ventricle until trabecular muscle could be visualized. For histological analysis, 50 μm cryosections were mounted with Fluoromount G. Images from all multicolour samples were acquired using a Leica SP5 AOBS microscope equipped with ×20 (0.7 NA) and ×40 (1.25 NA) objectives. Antibodies were not used to enhance fluorescence. 458 nm, 515 nm and 561 nm lasers were used to excite CFP, YFP and RFP, respectively. Each channel was acquired sequentially and imported into ImageJ, where channels were overlaid. Uniform contrast and brightness adjustments were made using Adobe Photoshop. To visualize the entire outer surface area, images were joined using Photoshop. To quantify the clone area, the size of a given clone in μm^2 was traced using ImageJ software. The percentage area occupied by a clone was calculated by dividing its measured area by the total surface area of both sides of the ventricle.

Full Methods and any associated references are available in the online version of the paper at www.nature.com/nature.

Received 8 January; accepted 15 March 2012.

1. Livet, J. *et al.* Transgenic strategies for combinatorial expression of fluorescent proteins in the nervous system. *Nature* **450,** 56–62 (2007).

2. Zhou, Y. *et al.* Latent TGF-β binding protein 3 identifies a second heart field in zebrafish. *Nature* **474,** 645–648 (2011).
3. Kikuchi, K. *et al. tcf21*$^{+}$ epicardial cells adopt non-myocardial fates during zebrafish heart development and regeneration. *Development* **138,** 2895–2902 (2011).
4. Cai, C. L. *et al.* Isl1 identifies a cardiac progenitor population that proliferates prior to differentiation and contributes a majority of cells to the heart. *Dev. Cell* **5,** 877–889 (2003).
5. Zhou, B. *et al.* Epicardial progenitors contribute to the cardiomyocyte lineage in the developing heart. *Nature* **454,** 109–113 (2008).
6. Meilhac, S. M., Esner, M., Kelly, R. G., Nicolas, J. F. & Buckingham, M. E. The clonal origin of myocardial cells in different regions of the embryonic mouse heart. *Dev. Cell* **6,** 685–698 (2004).
7. Keegan, B. R., Meyer, D. & Yelon, D. Organization of cardiac chamber progenitors in the zebrafish blastula. *Development* **131,** 3081–3091 (2004).
8. Stainier, D. Y., Lee, R. K. & Fishman, M. C. Cardiovascular development in the zebrafish. I. Myocardial fate map and heart tube formation. *Development* **119,** 31–40 (1993).
9. Mikawa, T., Borisov, A., Brown, A. M. & Fischman, D. A. Clonal analysis of cardiac morphogenesis in the chicken embryo using a replication-defective retrovirus. I. Formation of the ventricular myocardium. *Dev. Dyn.* **193,** 11–23 (1992).
10. Meilhac, S. M. *et al.* A retrospective clonal analysis of the myocardium reveals two phases of clonal growth in the developing mouse heart. *Development* **130,** 3877–3889 (2003).
11. Kikuchi, K. *et al.* Primary contribution to zebrafish heart regeneration by *gata4*$^{+}$ cardiomyocytes. *Nature* **464,** 601–605 (2010).
12. de Pater, E. *et al.* Distinct phases of cardiomyocyte differentiation regulate growth of the zebrafish heart. *Development* **136,** 1633–1641 (2009).
13. Auman, H. J. *et al.* Functional modulation of cardiac form through regionally confined cell shape changes. *PLoS Biol.* **5,** e53 (2007).
14. Hami, D., Grimes, A. C., Tsai, H. J. & Kirby, M. L. Zebrafish cardiac development requires a conserved secondary heart field. *Development* **138,** 2389–2398 (2011).
15. Lazic, S. & Scott, I. C. Mef2cb regulates late myocardial cell addition from a second heart field-like population of progenitors in zebrafish. *Dev. Biol.* **354,** 123–133 (2011).
16. Hu, N., Yost, H. J. & Clark, E. B. Cardiac morphology and blood pressure in the adult zebrafish. *Anat. Rec.* **264,** 1–12 (2001).
17. Liu, J. *et al.* A dual role for ErbB2 signaling in cardiac trabeculation. *Development* **137,** 3867–3875 (2010).
18. Poss, K. D., Wilson, L. G. & Keating, M. T. Heart regeneration in zebrafish. *Science* **298,** 2188–2190 (2002).
19. Wang, J. *et al.* The regenerative capacity of zebrafish reverses cardiac failure caused by genetic cardiomyocyte depletion. *Development* **138,** 3421–3430 (2011).
20. Jopling, C. *et al.* Zebrafish heart regeneration occurs by cardiomyocyte dedifferentiation and proliferation. *Nature* **464,** 606–609 (2010).
21. Snippert, H. J. *et al.* Intestinal crypt homeostasis results from neutral competition between symmetrically dividing Lgr5 stem cells. *Cell* **143,** 134–144 (2010).
22. Klein, A. M., Nakagawa, T., Ichikawa, R., Yoshida, S. & Simons, B. D. Mouse germ line stem cells undergo rapid and stochastic turnover. *Cell Stem Cell* **7,** 214–224 (2010).
23. Lopez-Garcia, C., Klein, A. M., Simons, B. D. & Winton, D. J. Intestinal stem cell replacement follows a pattern of neutral drift. *Science* **330,** 822–825 (2010).
24. Doupé, D. P., Klein, A. M., Simons, B. D. & Jones, P. H. The ordered architecture of murine ear epidermis is maintained by progenitor cells with random fate. *Dev. Cell* **18,** 317–323 (2010).

Supplementary Information is linked to the online version of the paper at www.nature.com/nature.

Acknowledgements We thank K. Kikuchi for generating *cmlc2:CreER* animals and for advice; J. Burris, A. Eastes, P. Williams and N. Blake for zebrafish care; A. Dickson for artwork; B. Hogan and Poss laboratory members for comments on the manuscript; and S. Johnson and Y. Gao for imaging advice. V.G. was supported by a National Heart, Lung, and Blood Institute (NHLBI) Medical Scientist Training Program supplement. K.D.P. is an Early Career Scientist of the Howard Hughes Medical Institute. This work was supported by grants from NHLBI (HL081674) and American Heart Association to K.D.P.

Author Contributions V.G. and K.D.P. designed experimental strategy, analysed data, and prepared the manuscript. V.G. performed all of the experiments.

Author Information Reprints and permissions information is available at www.nature.com/reprints. The authors declare no competing financial interests. Readers are welcome to comment on the online version of this article at www.nature.com/nature. Correspondence and requests for materials should be addressed to K.D.P. (kenneth.poss@duke.edu).

METHODS

Zebrafish and transgenic lines. Wild-type or transgenic zebrafish of the EK/AB background were used for all experiments and maintained at 3 fish per litre starting at 28 dpf. Water temperature was maintained at 26 °C for animals after 1 wpf. Ventricular resection surgeries were performed as described previously[18], removing approximately 20% of the ventricle at the apex. Published transgenic strains used in this study were (*Tg(cmlc2:CreER)*^{pd10})[11], (*Tg(gata5:loxP-mCherry-STOP-loxP-nucEGFP)*^{pd40})[11], (*Tg(cmlc2:EGFP)*^{f1})[25], (*Tg(cmlc2:nucDsRed2)*^{f2})[25] and (*Tg(β-actin:HRAS-EGFP)*^{vu119})[26]. Experiments with zebrafish were approved by the Institutional Animal Care and Use Committee at Duke University.

Construction of *priZm*. The Brainbow 1.0L plasmid was digested with NheI and partially digested with NotI to obtain the entire cassette, and subcloned downstream of the 9.8 kb zebrafish *β-actin 2* promoter from the *β-act2:RSG* construct[11]. The resulting plasmid was linearized by I-SceI digestion and injected into one-cell zebrafish embryos. RFP is the initial reporter cassette and default expression state from this construct. Two paired sites, *lox2272* and *loxP*, exist in the construct, which enable Cre-recombinase-mediated switching to expression of either CFP or YFP.

Thirty founder lines were isolated, and *Tg(β-act2:Brainbow1.0L)*^{pd49} was used for this study. The zebrafish *β-actin 2* promoter does not drive expression in epicardial or endocardial cells[11], facilitating clear visualization of *priZm* cardiomyocytes.

4-HT labelling. For 4-HT labelling of *cmlc2:CreER*; *priZm* embryos, 2 dpf embryos were placed in egg water with 4-HT added to a final concentration of 4 μM, from a 1 mM stock made in 100% ethanol. Embryos were treated for 6 h, rinsed once, and placed in fresh egg water. This labelling protocol was highly reproducible and induced recombination and appearance of diverse, non-red colours on half of the ventricular surface, calculated by digital quantification of red and non-red surface areas from whole-mount images of 30 dpf ventricles (50.0%; $n = 10$). By contrast, increased or reduced presence of 4-HT led to higher and lower recombination frequencies, respectively, which each reduced colour diversity.

For labelling of *cmlc2:CreER*; *priZm* juveniles at 30 dpf, animals were incubated in 1 μM 4-HT in aquarium water for 3 h. To specifically label trabecular muscle at 30 dpf, animals were incubated in 0.25 μM 4-HT for 1 h.

Imaging. Hearts were extracted at the indicated time points and fixed in 4% paraformaldehyde. After rinsing, the atrium was removed and the ventricle was placed on a coverslip in Fluoromount G. Another coverslip was used to compress the ventricle, allowing imaging of both ventricular surfaces. For surface images of whole-mounted ventricles, the z-position was adjusted until only surface muscle was visible. For confocal slices through whole-mounted hearts, the z-position was adjusted through the ventricle until trabecular muscle could be visualized. For histological analysis, 50 μm cryosections were mounted with Fluoromount G. Images from all multicolour samples were acquired using a Leica SP5 AOBS microscope equipped with ×20 (0.7 NA) and ×40 (1.25 NA) objectives. Antibodies were not used to enhance fluorescence. 458 nm, 515 nm and 561 nm lasers were used to excite CFP, YFP and RFP, respectively. Each channel was acquired sequentially and imported into ImageJ, where channels were overlaid. Uniform contrast and brightness adjustments were made using Adobe Photoshop. To visualize the entire outer surface area, images were joined using Photoshop. To quantify the clone area, the size of a given clone in μm^2 was traced using ImageJ software. The percentage area occupied by a clone was calculated by dividing its measured area by the total surface area of both sides of the ventricle.

Embryonic cardiomyocyte assays. *cmlc2:nucDsRed2*; *cmlc2:EGFP* double transgenic animals were raised to 3 dpf, fixed, sectioned at 30 μm, and stained with an antibody to DsRed2. Confocal stacks of the entire heart from each embryo were taken, and the number of myocytes within the ventricular wall was determined from three-dimensional projections generated using Imaris. To determine effects of 4-HT on cardiomyocyte proliferation, we treated 2 dpf embryos with 4 μM 4-HT for 6 h and fixed at 3 dpf. Ten-micrometre sections were stained with Mef2 and PCNA as described[27], and cardiomyocyte proliferation indices for each group were calculated from three ventricular sections. The numbers of $Mef2^+$ and $Mef2^+/PCNA^+$ cells were manually counted with the aid of ImageJ software.

Colour combinations and clone size. To examine the possibility that recombined colour combinations had differential effects on cardiomyocyte proliferation, we examined colour diversity in the largest and smallest cortical clones of 90 dpf ventricles that were labelled at 2 or 30 dpf. From 21 ventricles, 16 unique colours were represented in the 21 large basal clones. Seventeen unique colours were represented in 21 of the smallest clones. Individual colours were observed in both small and large clone groups, including two shades of grey (in which the clone is expressing all three fluorescent proteins). This distribution was consistent with the idea that colour combinations do not have adverse effects on proliferative ability.

25. Burns, C. G. *et al.* High-throughput assay for small molecules that modulate zebrafish embryonic heart rate. *Nature Chem. Biol.* **1,** 263–264 (2005).
26. Cooper, M. S. *et al.* Visualizing morphogenesis in transgenic zebrafish embryos using BODIPY TR methyl ester dye as a vital counterstain for GFP. *Dev. Dyn.* **232,** 359–368 (2005).
27. Kikuchi, K. *et al.* Retinoic acid production by endocardium and epicardium is an injury response essential for zebrafish heart regeneration. *Dev. Cell* **20,** 397–404 (2011).